

International Journal of Scientific Research and Reviews

Thermal conductivity and its finite-size scaling in 2D He-4 system

Md. Rafiquezaman Ansari^{1*} and S. Nadim Asghar²

¹Department of Physics, Maulana Azad College of Engineering & Technology, Patna 801113, India

²Department of Physics, J. P. University, Chapra 841301, India

ABSTRACT

We present the theoretical study of thermal conductivity and its finite-size scaling in 2D He-4 system. This paper describes the expected behavior of the system if it is assumed that finite-size scaling is valid for the conductivity. The predicted scaling function is used to obtain a quantitative assessment of the gravity effect on Earth-based measurements for different L and typical sample thickness (height) h . The KA results showed that the thermal resistivity $R=1/\lambda$ in the cylindrical geometry remains finite at T_λ , and decays exponentially as the temperature T is reduced below T_λ . The data confirms that there is no phase transition in the one-dimensional system, as had been expected on general theoretical grounds.

KEYWORDS: Thermal conductivity, Finite-size scaling in 2D He-4 system, Phase transition

***Corresponding author**

Dr. Md. Rafiquezaman Ansari

Department of Physics,

Maulana Azad College of Engineering & Technology,

Patna 801113, India

Email: azamsaba27@gmail.com MobNo. -9934258814

INTRODUCTION

An interesting issue in condensed-matter physics is the nature of the interface between solids and fluids. The microscopic aspects of systems near boundaries are difficult to study. However, when the fluid is near a critical point, the boundary layer adjacent to the solid surface acquires a macroscopic thickness. When the fluid phase is of limited spatial extent, the boundary will influence significantly the average macroscopic properties of the system. Thus, a critical fluid system which is confined can be used to study boundary effects. In addition to these “surface” effects, a system confined in a finite geometry will also exhibit “bulk” finite-size effects; both contributions are expected to be describable within the general context of finite-size scaling¹ and by specific calculations based on the renormalization-group theory (RGT)², and we will collectively refer to them as “finite-size effects”.

There is a long history of experimental work on finite-size effects on equilibrium properties near T_λ . However, so far all of this work has been restricted to saturated vapor pressure (SVP). Much of the older work was carried out in poorly defined geometries with a significant distribution of characteristic sizes such as found in packed powders, making it difficult to interpret the results quantitatively in terms of modern theories. More recently measurements have been made in more uniform geometries of better known dimensions³⁻⁷.

The interpretations of these results are in part in conflict with theoretical predictions based on scaling arguments and RGT considerations. Thus there is a strong need for additional accurate measurements over a wide range of the pressure P and of the size L or precisely known and uniform geometries. Systems with confinement in one, two, and three dimensions, corresponding to parallel-plate, cylindrical, or cubic geometries respectively, are expected to represent three different universality classes and need to be investigated. Experiments on transport properties in manifestly finite geometries are almost non-existent. Here at least three cases can realistically be investigated. In parallel-plate geometry one could have the heat flow \bar{Q} parallel or orthogonal to the plates. In a cylindrical geometry \bar{Q} most likely would be in the axial direction. Qualitatively different finite-size effects would be expected for the three cases. The most relevant measurements we know the ones of the thermal conductivity λ carried out by Kahn and Ahlers⁸ (KA) on He-4 at SVP. Their sample was contained in the long, narrow tubes of a glass capillary array (GCA) (also known as micro-channel plates) and thus represents the cylindrical geometry with axial heat flow. The tube radius L was 1 μm . The major goal of the flight-definition project “Boundary Effects on transport properties and dynamic finite-size scaling near the Super fluid Transition line of 4He” (BEST) is to provide data for

λ in the same geometry over a wide range of L and P . Plans for this work will build upon the Admeasurements and the assumption of finite-size scaling.

This paper describes the expected behavior of the system if it is assumed that finite-size scaling is valid for the conductivity. The expected scaling function is exploited to find a quantitative valuation of the gravity effect on Earth-based measurements for different L and typical sample thickness (height) h and to The KA results indicated that the thermal resistivity $R = 1/\lambda$ in the cylindrical geometry remains finite at T_λ , and decays exponentially as the temperature T is decreased below T_λ . The data confirm that there is no phase transition in three-dimensional system, as had been expected on general theoretical grounds.

Important as these results may be, by themselves they are not adequate to test the ideas of finite-size scaling for transport properties because the dependence upon the characteristic size L of the geometry is at issue and measurements over a wide range of L are required. They also do not explore the expected universality of the corresponding scaling function along the λ -line as a function of pressure. Thus the significance of the $1 \mu\text{m}$ data would be enormously enhanced by equivalent results for different characteristic sizes and over a range of P . It turns out that a significant range of L can be explored only by extending it to relatively large values. However, for $L \geq 8 \mu\text{m}$ the effect of Earth's gravity⁹ prevents definitive measurements and experiments are feasible only in microgravity.

THEORETICAL ANALYSIS

A quantitative analysis of the conductivity $\lambda(t, L)$ of the finite system requires a quantitative knowledge of $\lambda(t) = \lambda(t, \infty)$ for the bulk system. The dependence upon t of the bulk conductivity, although complicated, is already remarkably well understood both experimentally¹⁰⁻¹⁴ and theoretically¹⁵. There do remain some unresolved issues, however, which are of interest for their own sake as well as important to the quantitative interpretation of $\lambda(t, L)$.

In Fig. 1 we show λ against $t \equiv T/T_\lambda - 1$ on logarithmic scales for saturated vapor pressure (SVP) and for $P = 28$ bar. Similar results exist at several intermediate pressures, but are omitted here for clarity. For sufficiently small t , the data to a good approximation fall on straight lines, and thus can be described by the power law

$$\lambda = \lambda_0 t^{-x} \quad (1)$$

However, on closer inspection one finds that the exponent

$$x \equiv \frac{d[\ln(\lambda)]}{d[\ln(t)]} \quad (2)$$

But the exponent is an effective exponent which depends very slightly upon t . Furthermore, on theoretical grounds one would have expected x to have a universal asymptotic value equal or close to $\nu/2$, which on the basis of second-sound-velocity measurements has a value near 0.3352^{16} . However, measurements of λ give a slightly pressure dependent effective value which varies from $x \cong 0.44$ at SVP to $x \cong 0.41$ at 28 bar. This was explained quantitatively nearly two decades ago by detailed RGT calculations of non-universal (i.e. pressure dependent) non-asymptotic contributions to λ^{15} . The quantitative explanation of the rather complicated behavior of $\lambda(t, P)$ along the entire transition line $T_\lambda(P)$ is a major success of the RGT. However, the comparison between experiment and theory still has its limitations, as can be seen from the range of the data in Fig. 1. The data are only for $t \geq 3 \times 10^{-6}$. For transport properties this is a more severe limitation than for equivalent results for equilibrium properties because the critical region where approximate power law dependence is found is much narrower. As seen in Fig. 1, at SVP this region is $t \leq 10^{-3}$. The range becomes even narrower at higher pressure, being confined to $t \leq 10^{-4}$ at 28 bar. Thus it would be extremely useful to extend the range to smaller t to provide a more stringent test of the theory.

Some extension of the range can actually be obtained on Earth with the use of high-resolution thermometry¹⁷; but for $t \leq 10^{-7}$ gravity would prevent measurements from being made⁹. In a microgravity environment, this range could be extended by another decade or two. This is particularly important because recent high-resolution measurements¹⁸ at vapor pressure have suggested a departure from the RGT prediction for $t \leq 10^{-6}$. It is also important for the unambiguous determination of the finite-size contribution for the large values $L = 25$ or $50 \mu\text{m}$ envisioned for the microgravity experiment. Thus a secondary objective of BEST was to obtain high-quality data of the bulk conductivity along several isobars for $t \leq 10^{-8}$ or so.

At present, the RGT is not sufficiently advanced to provide predictions of the critical behavior of transport properties in a confined geometry near T_λ of He-4²⁰. Thus we can describe the anticipated results only within the general context of phenomenological scaling arguments. Although scaling has been used for finite-size effects on static properties, there is at present no experimental foundation for its application to transport properties. Thus our work will provide the theoretical study of finite-size scaling for the dynamics. To formulate the problem more precisely, we assume that $\lambda(t)$ can be written in the form of Eq. (1). This approximation is justified to the extent to which the

data close to T_λ in Fig. 1 fall on straight lines. For the finite system we will find it more convenient to discuss the thermal resistivity $R(t, L) = 1/\lambda(t, L)$ because the difference between it and $R(t) = R(t, \infty)$ remains finite.

For the cylindrical geometries, we will simply take L to be equal to the cylinder radius. In that case the finite-size effect well above T_λ , where surface effects dominate, should on geometrical grounds be the same as for parallel plates with spacing L and with \tilde{Q} parallel to the plates because the ratio of the surface area to the cross sectional area is the same. However, near and below T_λ qualitatively different behavior would be expected for the two cases. Regardless of the geometry, and in analogy to static scaling arguments, we expect the relationship between $R(t, L)$ and $R(t)$ to be given by a function only of L/ξ where

$$\xi = \xi_0 t^{-\nu} \tag{3}$$

with $\nu = 0.6705$ [20] is the bulk correlation length above T_λ .

Thus we write $R(t)$ in terms of $\xi(t)$ as

$$R(t) = R_0 \xi_0^{x/\nu} \xi^{-x/\nu} \tag{4}$$

and make the Ansatz

$$R(t, L) = R(t) \tilde{F}\left(\frac{L}{\xi}\right) \tag{5}$$

This appears reasonable above T_λ , but below the transition where $R(t) = 0$, it is not obvious that this will lead to a meaningful expression. Proceeding nonetheless, we find after some rearrangement the scaling function

$$F(X) = \frac{R(t, L)}{R_0} \left(\frac{L}{\xi_0}\right)^{x/\nu} \tag{6}$$

with

$$X = \left(\frac{L}{\xi_0}\right)^{1/\nu} |t| \tag{7}$$

Equivalently, one can obtain

$$G(X) = \frac{R(t, L) - R(t)}{R_0} \left(\frac{L}{\xi_0}\right)^{x/\nu} \tag{8}$$

Above T_λ the function $G(X)$ is more sensitive to the finite-size effect since the bulk resistivity is subtracted; but below the bulk transition $R(t)=0$ and thus $G(X)$ is the same as $F(X)$.

The most appealing result would be to find that the functions $F(X)$ and $G(X)$ are universal, implying that (for a given geometry) they do not depend on L and P . We believe that this universality is particularly uncertain below T_λ where $R(t) \equiv 0$. Our concern is enhanced by the fact that (at least for the cylindrical geometry) $R(t,L) - R(t)$ has a very different dependence upon t above and below T_λ . Above the transition, where the difference is expected to be determined by surface effects, experiment suggests that it varies as $t^{-\nu}$. However, below T_λ the difference decays exponentially as $|t|$ increases. This behavior suggests that the physical phenomena which dominate the finite-size effects on the two sides of the transition are quite different from each other. The exponential dependence below T_λ suggests that the physics of the super fluid phase comes into play in a crucial way, perhaps in the form of phase-slip phenomena such as in one-dimensional superconductors. Of course this does not exclude the possibility that the finite-size effects on both sides scale with ξ , and that the functions F and G which we have defined are nonetheless universal. Clearly an experimental determination of F and G at several values of L and P will be extremely instructive. It is to be expected that the functions $F(X)$ and $G(X)$ as defined by Eqs. (6) to (8) will be found to be pressure dependent, and thus apparently non-universal. This is so because the simple power law description which we have assumed for $R(t)$, although it fits the data extremely well, is inconsistent with universality because the effective exponent x depends on P . A more complete theory, based on a universal asymptotic $R(t)$ and the known non-universal non-asymptotic corrections, might recover the expected universality as a function of pressure. However, such a theory does not appear to exist at this time. Thus we are at present unable to make quantitative predictions of the pressure dependence of the finite-size effect. However, we expect that the determination at SVP of the function $G(X)$ for the excess resistivity should still be valid to a reasonable approximation even at the higher pressures.

The main purpose of the planned work is to determine whether $R(t,L)$ for the cylindrical geometry can indeed be written in the form of Eqs. (6) and (8), and to determine whether the functions $F(X)$ and $G(X)$ are universal, i.e. independent of L and P . This will be possible only when data become available along several isobars over a significant range of L and of t . There are several factors which restrict the range of L which can be used. One of them is the practical issue of the

availability of suitable geometries. Commercially one has not been able to obtain GCA's with capillary radii smaller than $0.5 \mu\text{m}$. However, even if one were to produce smaller capillaries, they would be only of limited use. The reason for this is that a comparison with theory will be easiest in the range of t where the bulk system shows a strong power law divergence. This range often is referred to as the "critical region". It is known that the correlation-length amplitude ξ_0 is only weakly dependent on pressure²¹. Thus one expects a given L to produce a finite-size-affected range of t which is nearly pressure independent. On the other hand, from Fig. 1 it is clear that the critical region for the dynamics is strongly pressure dependent. At high pressure it is restricted to $t \leq 3 \times 10^{-4}$, whereas at vapor pressure it covers the range $t \leq 3 \times 10^{-3}$. Thus it is desirable to use geometries with characteristic capillary radii which are large enough for the finite-size effects to occur for $t \leq 3 \times 10^{-4}$. Examination of the $1 \mu\text{m}$ data (see below) shows that the finite-size region extends over the range $t \leq 10^{-4}$.

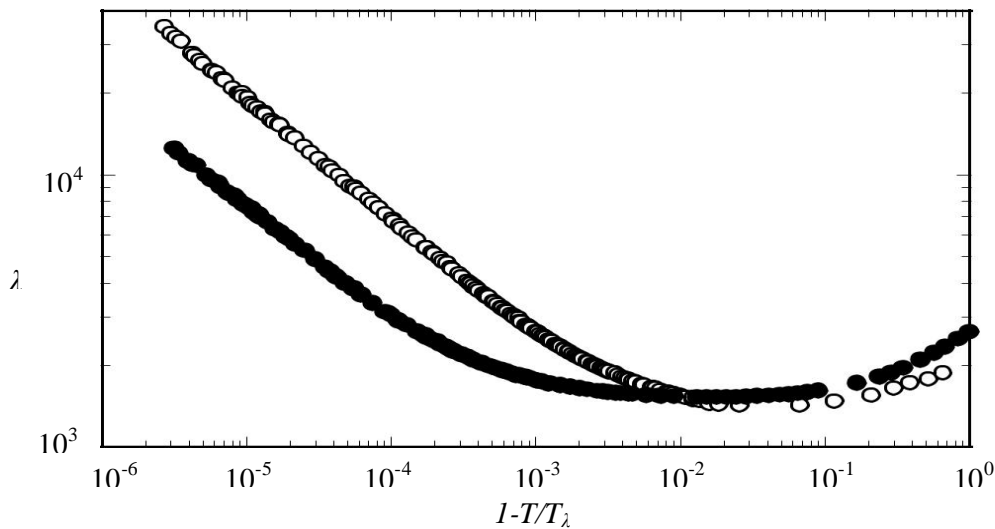


Fig. 1. The thermal conductivity of He-4 above T_λ as a function of the reduced temperature [14] at vapor pressure (open symbols) and at 28 bar (solid symbols). The results are shown on logarithmic scales.

Assuming the scaling of Eq. 6, we conclude that the finite-size region will be about as wide as the critical region at the higher pressures when $L \cong 0.5 \mu\text{m}$, and that the amount of useful information obtainable diminishes as L decreases below half a μm . Thus our only real option for covering a wide range of L is to go to large L . However, for large L the finite-size effects of interest occur very

close to T_λ where the sample in homogeneity due to the Earth's gravitational acceleration has a significant influence.

The gravity effect is illustrated in Fig. 2 in terms of the phase diagram of He-4. The λ line, along which the liquid undergoes a transition from a super fluid (He-II) to a normal (Navier-Stokes) liquid (He-I), extends from 2.172 K at vapor pressure (0.05 bar) to 1.763 K at the melting pressure (30.13 bar)^{21, 22}. The in homogeneity induced by gravity⁹ is due to the hydrostatic pressure which varies with height in the liquid. This pressure variation has the effect of inducing a vertical spatial variation of the transition temperature. This is illustrated in more detail in the right portion of Fig. 2. If the sample top is at a pressure $P = P_0$, then the bottom will be at $P = P_0 + \rho gh$ where ρ is the fluid density, g the gravitational acceleration, and h the sample height. Over this pressure the transition temperature $T_\lambda(P)$ varies significantly. The parameter $\beta = -(\partial T / \partial z)_\lambda$ is

$$\beta = -\rho g \left(\frac{\partial T}{\partial z} \right)_\lambda \quad (9)$$

This provides a quantitative measure of the severity of the gravity effect. Values of $\beta(P)$, in $\mu\text{K}/\text{cm}$, are given in Fig. 3. One sees that, for a typical sample of size 1 cm at SVP, one has a two-phase region over a temperature interval of 1.27 μK . Thus it is not possible to approach the transition more closely on average than within a μK or so. At higher pressures $\beta(P)$ increases because the slope of the λ -line $(\partial P / \partial T)_\lambda$ decreases and the density increases. At 30 bar the two-phase region for a sample of a given height would be wider by a factor of 2.5. Of course the effect of gravity on the average measured properties extends well beyond the two-phase region.

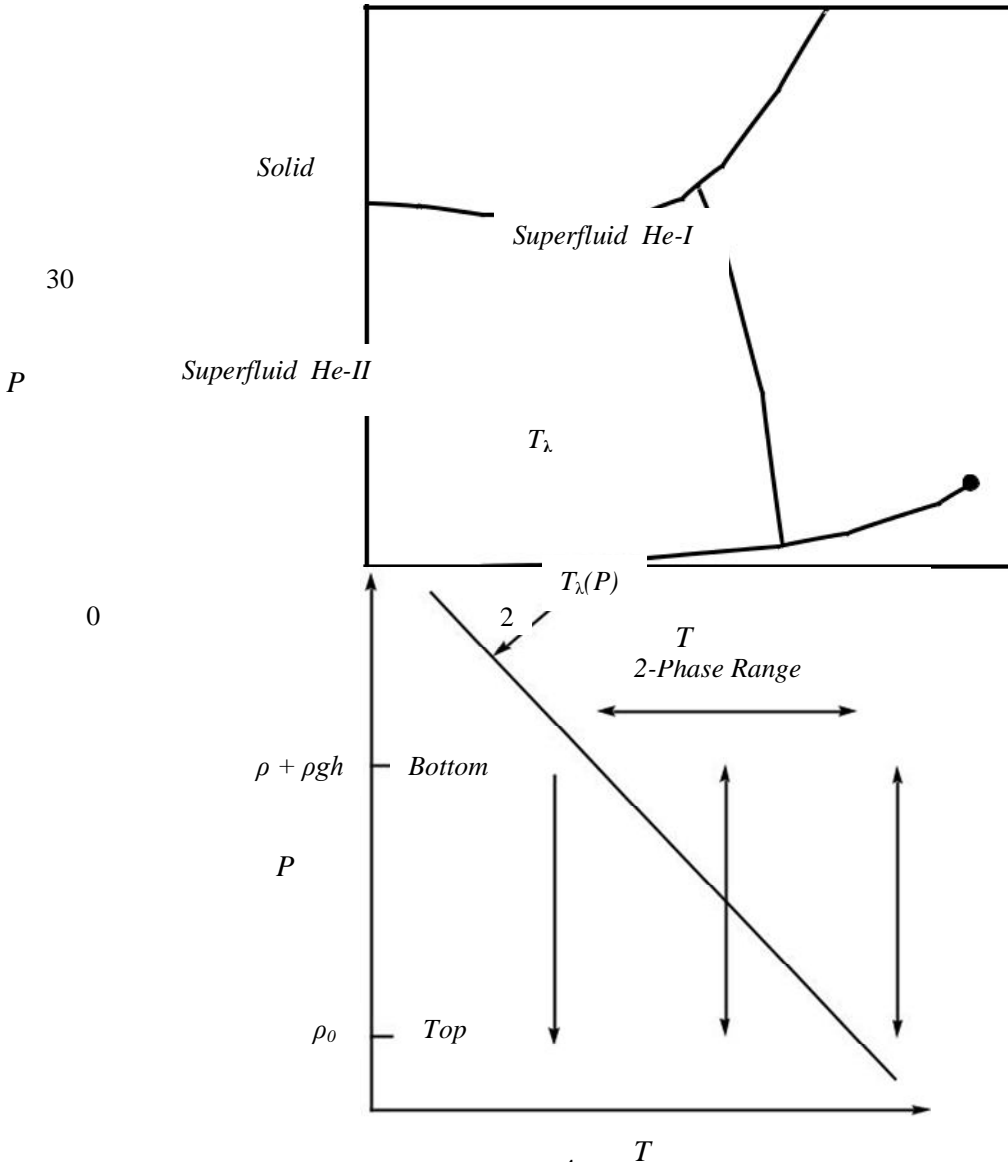


Fig. 2. Schematic phase diagram of ^4He , and an illustration of the gravity effect.

Associated with the distribution of transition temperatures is a more subtle “averaging” over a vertical range ξ_g of the properties due to the growth of the correlation length near the local transition. Thus the local properties are no longer those of the three-dimensional bulk transition. For most experiments it is smaller than the effect due to the variation of $T_\lambda(z)$ over the sample height h . Returning to the finite-size samples, it turns out that helium at SVP and in cylinders with $L \geq 8 \mu\text{m}$ can not be studied effectively on Earth because the gravitational “rounding” of the resistivity will become significant compared to the expected finite-size rounding. At $P = 30 \text{ bar}$, gravitational rounding becomes a problem already for $L \cong 3.5 \mu\text{m}$. In microgravity the maximum useable size is

limited only by the experimental temperature resolution, and is near 50 μm . Thus the microgravity experiment can add a factor of 6 to 14 in L (depending on the pressure) to the size range accessible on Earth. We note that a factor of 6 (14) in L is a factor of 15 (50) for the scaling variable X .

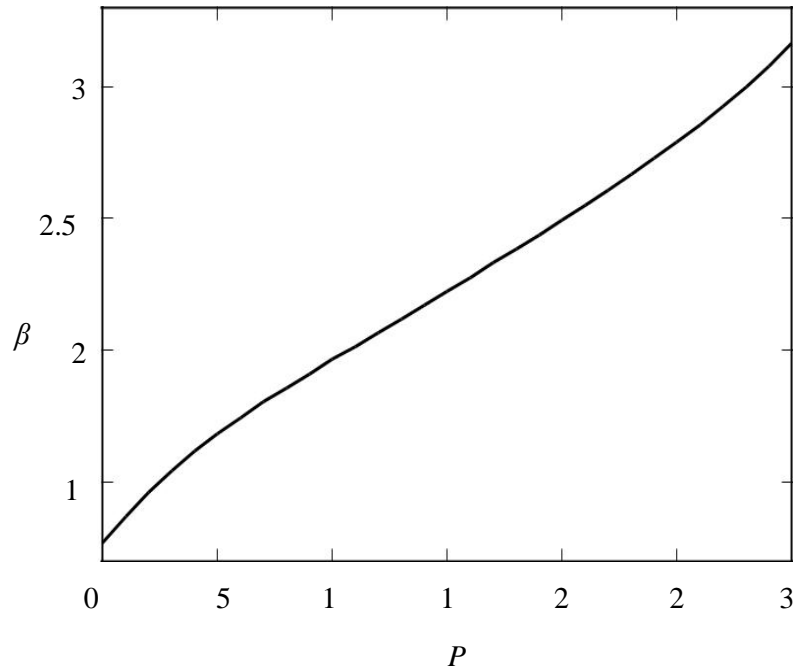


Fig. 3. The width per cm of sample height of the temperature range of isothermal coexistence of He-I and He-II (the two-phase region) as a function of the pressure.

DATA ANALYSIS AND DISCUSSION

An effective evaluation of the finite-size thermal conductivity of ^4He near T_λ requires an accurate knowledge of the bulk conductivity λ . The bulk conductivity was measured by several authors¹⁰⁻¹³. We will use the data in¹² for their “Cell F” (TA) because they cover a very wide range of reduced temperatures, and because they are the only set we know of which covers several isobars in addition to saturated vapor pressure (SVP). The SVP and 28 bar data for λ were shown already in Fig. 1 over a wide range of t . They extend from $t \cong 3 \times 10^{-6}$ to $t \cong 1.0$. The large- t data are necessary for the evaluation of the finite-size data because the bulk and finite-size measurements must be normalized to each other in a region where finite-size effects are negligible. For small t the bulk data are shown in the form of the resistivity on logarithmic scales in Fig. 4. Deviations from fits of the power law

$$R = R_0 t^x \tag{10}$$

to these data are shown in Fig. 5. The fits yielded the parameters

$$R_0 = 8.312 \times 10^{-3} \text{ cm K s / erg}, \quad x = 0.4397 \quad (11)$$

at saturated vapor pressure and

$$R_0 = 1.507 \times 10^{-2} \text{ cm K s / erg}, \quad x = 0.4127 \quad (12)$$

at $P = 28$ bar.

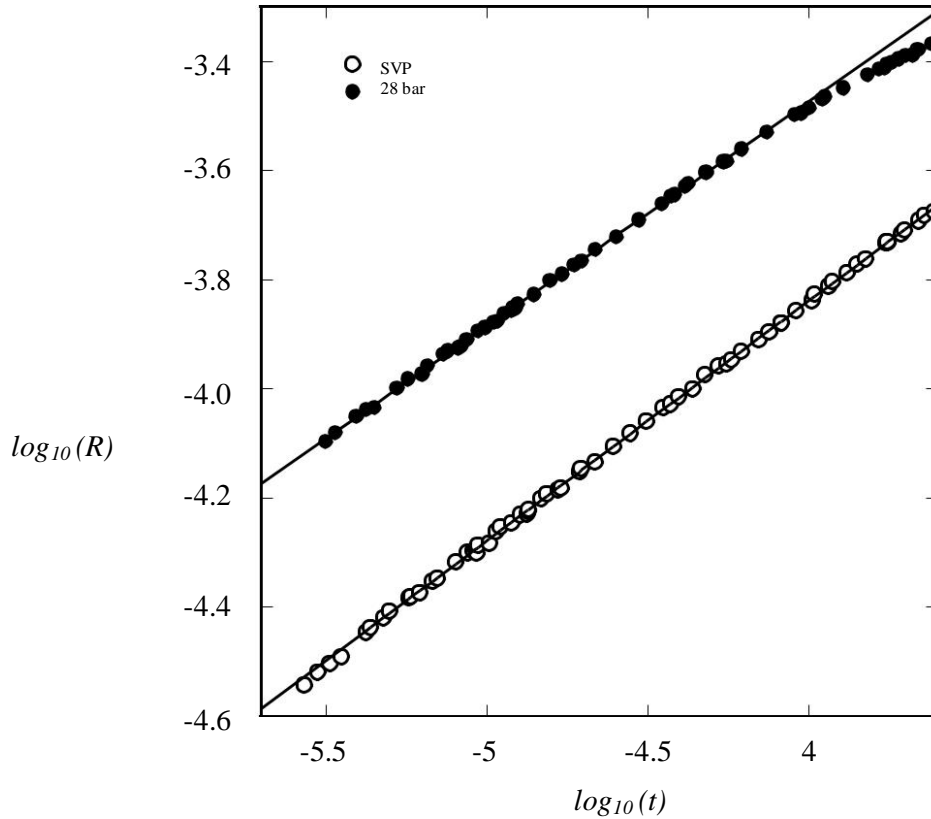


Fig. 4. The resistivity $R = 1/\lambda$ in the critical region for bulk helium at SVP (open circles) and at 28 bar (solid circles) on logarithmic scales. The solid lines are power law fits to the data for $t < 2 \times 10^{-4}$ at SVP and $t < 8 \times 10^{-5}$ at 28 bar.

An analysis at all pressures where measurements exist¹⁴ (0.05, 6.85, 14.73, 22.30, and 28.00 bar) yielded exponents which could, within their uncertainty, be represented by

$$x = 0.4395 - 0.000994P \quad (13)$$

where P has the units bar. Fits of the data with the exponent fixed at that given by Eq. (13) gave $R_0 = 0.00831, 0.00974, 0.01107, 0.01302, \text{ and } 0.01498 \text{ cm K s / erg}$ for the five isobars. In the calculations of finite-size and gravity effects given below we will use x as given by Eq. (13) and R_0 given by linear interpolation between the values given here.

The conductivity of He-4 at SVP in GCAs with capillary radii of 1 μm has been examined. It was not possible to determine the effective area of the helium with sufficient accuracy. In addition,

the parallel conduction through the cell wall, the glass, and the epoxy used to seal the GCA to the wall was not measured independently. Therefore the parallel conduction and the length-to-area ratio $h/A = 0.39 \text{ cm}^{-1}$ were obtained by adjusting them so as to cause the helium conductivity to agree with the TA data in the temperature range $7 \times 10^{-4} \leq t \leq 6 \times 10^{-3}$.

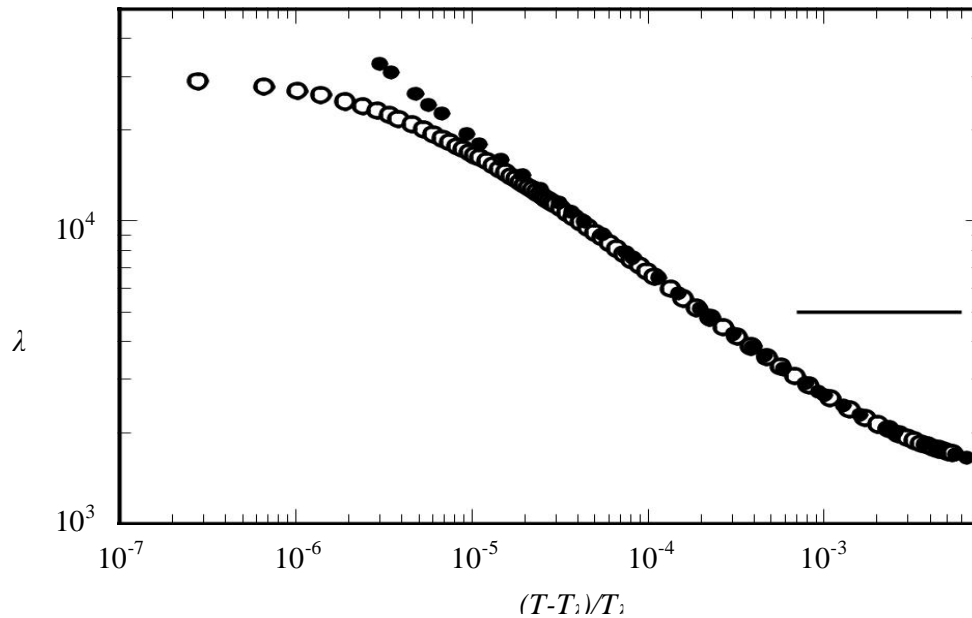


Fig. 5. The thermal conductivity at SVP for bulk helium (solid circles) and for helium in a GCA with pore radii of $1 \mu\text{m}$ (open circles). The horizontal bar shows the range of t over which the finite-size data were fit to the bulk data by adjusting the parallel (“wall”) conduction and the area-to-length ratio.

In this range, which is shown in Fig. 5 by the solid horizontal bar, the finite-size effect on λ is expected to be negligibly small. The results are shown over a wide range of t in Fig. 5. The solid circles are the TA bulk data, and the open circles are the results for the finite geometry. As T_λ is approached, the finite-size effect becomes apparent.

The data for the restricted geometry do not diverge like the bulk data, and instead approach a finite value as t vanishes. Data for R in the finite-size-affected region of t are shown on linear scales in Fig. 6. They reveal a rounded transition, with no evidence of a singularity, as would be expected for a one-dimensional system. Above T_λ the finite-size effect on R extends to quite large values of t . This is characteristic of the surface contribution to finite-size effects, as seen in static properties. Below T_λ ($t < 0$), $R(t, L)$ approaches zero rather more rapidly.

The behavior below T_λ is shown in more detail in Fig. 7. One sees that R reaches a finite value as t decreases. This saturation is due to the series resistance of the copper end plates of the

conductivity cell and to the series boundary resistance which had not been subtracted. It corresponds to an effective boundary resistivity $R_b = 2.1 \times 10^{-7}$ cm s K / erg. When R_b is subtracted, the data yield the dashed line in the figure. One sees that the dependence of R on t at low temperatures is consistent with an exponential decay of R as t decreases. The very rapid decrease of R with decreasing t permits its measurement only over a relatively narrow range of t . As a guide, the two horizontal dotted lines correspond to R_b and $2R_b$.

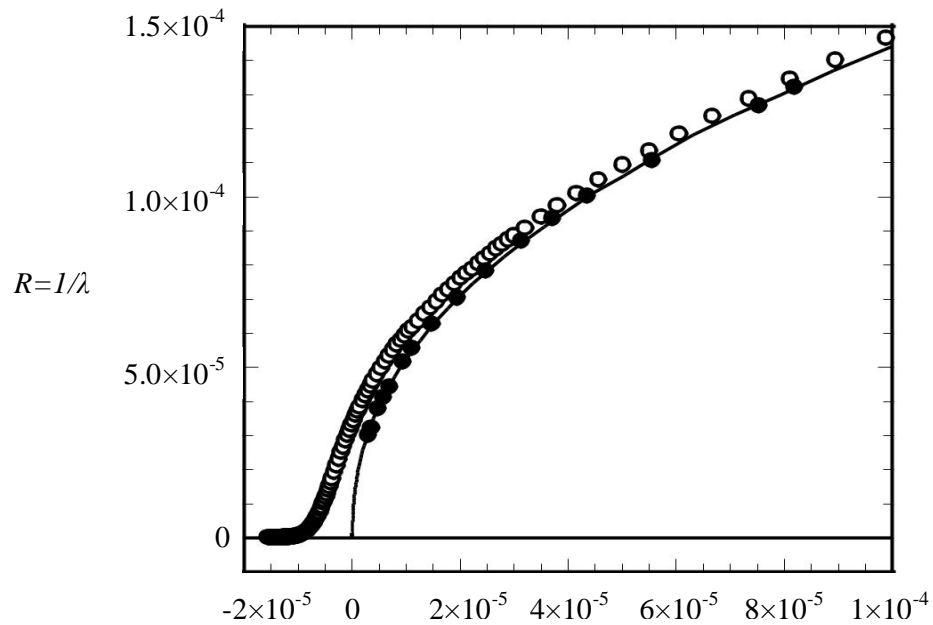


Fig. 6. The thermal conductivity at SVP for bulk helium (solid circles) and in a GCA with pore radii of 1 μ m (open circles) in the finite-size region on linear scales. The solid line is the fit Eqs. (10) and (11) to the bulk data.

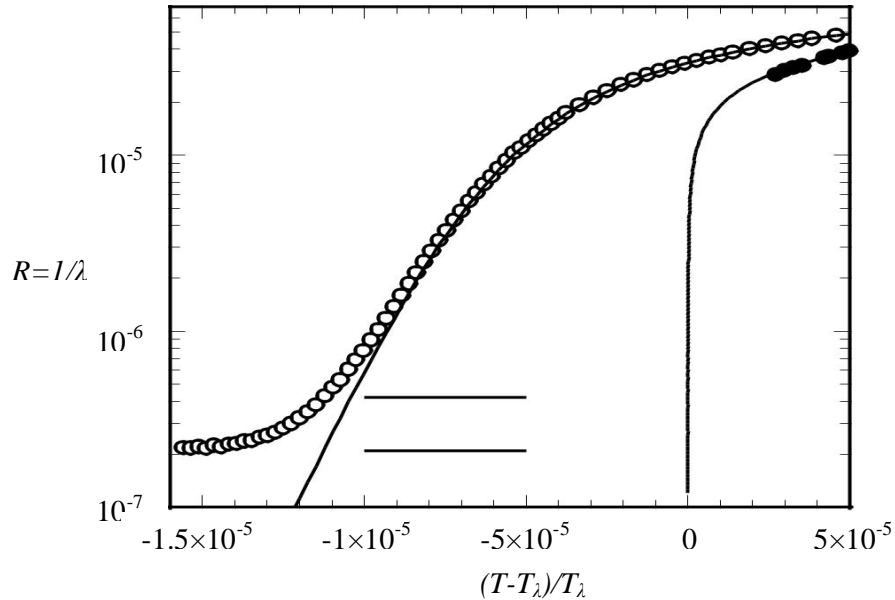


Fig. 7. The thermal resistivity R close to T_λ at SVP for bulk helium (solid circles) and for helium in a GCA with pore radii of $1 \mu\text{m}$ (open circles). The vertical scale is logarithmic and the horizontal one is linear. The solid line is the fit Eq. (10) to the bulk resistivity. The dashed line is $R(t, L)$ after subtraction of the boundary contribution.

At a reduced temperature -1.1×10^{-5} , $R(t, L)$ is about equal to R_b and for smaller t $R(t, L)$ soon ceases to be measurable. A fit of $R(t, L)$ (after the subtraction of R_b) to an exponential function gave

$$\frac{R}{R_d} = \exp\left(\frac{t}{t_0}\right) \quad (14)$$

with $R_d = 0.0052 \text{ s cm K / erg}$ and $t_0 = 1.1 \times 10^{-6}$. We note that in the assumed functional form Eq. (14) the argument of the exponential is linear in the absolute temperature T . Because of the narrow range of t over which the exponential decay of R can be measured, the data are not sufficient to rule out a somewhat different dependence upon T . Clearly it would be interesting to examine the behavior of R below T_λ theoretically, initially perhaps in the mean-field limit and in analogy to the known behavior of one-dimensional superconductors. A specific prediction could then be tested for consistency with the data. Of course it would be particularly interesting to see whether the scaling with ξ/L implied by Eq. (6) is consistent with the expected behavior.

CONCLUSION

In conclusion, the ground-based measurements of the thermal conductivity $\lambda(t, L)$ near the bulk super fluid-transition line $T_\lambda(P)$ of He-4 confined in cylindrical geometries with axial heat flow provides an evaluation of existing data near T_λ at SVP in cylinders of $L = 1 \mu\text{m}$ radius and uses these to derive a scaling function for the resistivity $R(t, L) = 1/\lambda(t, L)$. The scaling function is used to predict the conductivity for other values of L and P . These predictions are used to assess quantitatively the effect of gravity on potential Earth-based measurements. It is found that the gravity effect for R is particularly severe below T_λ .

REFERENCES

1. M. E. Fisher in Critical Phenomenon, Proc. 51st "Enrico Fermi" Summer School, Varenna, Italy, ed. M. S. Green Academic Press, NY, 1971;1.
2. Dohm V., "The super fluid transition in confined 4He: Renormalization-group theory" Phys. Script. 1993; T49: 46-58.
3. Chen TP and Gasparini FM, "Scaling of the Specific Heat of Confined Helium near T_λ " Phys. Rev. Lett. 1978; 40: 331-333.
4. Gasparini FM, Chen TP., and Bhattacharyya B, "Corrections to scaling and surface specific heat of confined helium" Phys. Rev. 1981; B 23: 5797-5814.
5. Rhee I, Gasparini FM., and Bishop DJ, "Finite-size scaling of the superfluid density of ^4He confined between silicon wafers" Phys. Rev. Lett. 1989; 63: 410-413.
6. Coleman M and Lipa JA, "Heat Capacity of Helium Confined to 8- μm Cylinders near the λ Point" Phys. Rev. Lett. 1995;74: 286-289.
7. Mehta S and Gasparini FM., "Specific heat and scaling of ^4He confined in a planar geometry" Phys. Rev. Lett. 1997; 78: 2596-2599.
8. Kahn AM and Ahlers G., "Thermal Conductivity of near the Super fluid Transition in a Restricted Geometry" Phys. Rev. Lett. 1995; 74: 944-947.
9. Ahlers G., "Effect of the Gravitational Field on the Super fluid Transition in He^4 " Phys. Rev. 1968 171: 275-282.
10. Ahlers, G., "Some aspects of the effect of gravity on the super fluid transition in ^4He Low Temp. Phys. ;1991; 84: 173-195.
11. Ahlers G., "Thermal Conductivity of He I Near the Super fluid Transition" Phys. Rev. Lett. 1968; 21: 1159-1162.

12. Kerrisk JF and Keller WE., "Thermal Conductivity of Fluid He-3 and He-4 at Temperatures between 1.5 and 4.0-degrees K and for Pressures up to 34 atm" Phys. Rev. 1969; 177: 341-351.
13. Tam WY and Ahlers G., "Thermal conductivity of ^4He I from near T_λ to 3.6 K and vapor pressure to 30 bars" Phys. Rev. 1985; B 32: 5932-5958.
14. Dingus M, Zhong F, and Meyer H, "Thermal transport properties in helium near the superfluid transition. I. ^4He in the normal phase" J. Low Temp. Phys. (1986) 65, 185-212 .
15. Tam WY and Ahlers G., "Thermal conductivity of ^4He I near T_λ from vapor pressure to 28 bars: comparison of experiment and theory" Phys. Rev. B (1986) 33, 183-196.
16. Dohm V., "Renormalization-group flow equations of model F" Phys. Rev. B (1991) 44, 2697-2712.
17. Goldner LS and Ahlers G., "Superfluid fraction of ^4He very close to T_λ " Phys. Rev. B (1992) 45, 13129-13132.
18. Chui TCP., Swanson DR, Adrians MJ, Nissen JA, and Lipa JA., "Temperature: its Measurement and Control in Science and Industry, edited by J.F. Schooly (American Institute of Physics, N.Y.,). 1992; 6
19. Lipa JA and Chui TCP., "High-resolution thermal-conductivity measurements near the lambda point of helium" Phys. Rev. Lett. 1987; 58:1340-1343.
20. Koch W, Dohm V, and Stauffer D. "Order-Parameter Relaxation Times of Finite Three-Dimensional Ising-like Systems", Phys. Rev. Lett. 1996; 77: 1789-1792.
21. Singhaas A and Ahlers G., "Universality of static properties near the super fluid transition in ^4He " Phys. Rev. B 1984; 30: 5103-5115.
22. Ahlers G., "Properties of He^4 Near the γ Phase" Phys. Rev. 1964; 135: 10-16.